Development 130, 209-220

doi:10.1242/dev.00181

DEVELOPMENT AND DISEASE

BMP signaling is required for septation of the outflow tract of the mammalian heart

Emmanuèle C. Délot[1,2,3], Matthew E. Bahamonde[1,4], Manxu Zhao[1] and Karen M. Lyons[1,4,5,*]

[1]Department of Orthopaedic Surgery, UCLA School of Medicine, Los Angeles, CA 90095, USA
[2]Department of Human Genetics, UCLA School of Medicine, Los Angeles, CA 90095, USA
[3]Department of Pediatrics, UCLA School of Medicine, Los Angeles, CA 90095, USA
[4]Department of Biological Chemistry, UCLA School of Medicine, Los Angeles, CA 90095, USA
[5]Department of Molecular Cell and Developmental Biology, UCLA, Los Angeles, CA 90095, USA
*Author for correspondence (e-mail: klyons@mednet.ucla.edu)

Accepted 1 October 2002

SUMMARY

Bone morphogenetic proteins (BMPs) constitute a family of ~20 growth factors involved in a tremendous variety of embryonic inductive processes. BMPs elicit dose-dependent effects on patterning during gastrulation and gradients of BMP activity are thought to be established through regulation of the relative concentrations of BMP receptors, ligands and antagonists. We tested whether later developmental events also are sensitive to reduced levels of BMP signaling. We engineered a knockout mouse that expresses a BMP type II receptor that lacks half of the ligand-binding domain. This altered receptor is expressed at levels comparable with the wild-type allele, but has reduced signaling capability. Unlike Bmpr2-null mice, mice homozygous for this hypomorphic receptor undergo normal gastrulation, providing genetic evidence of the dose-dependent effects of BMPs during mammalian development. Mutants, however, die at midgestation with cardiovascular and skeletal defects, demonstrating that the development of these tissues requires wild-type levels of BMP signaling. The most striking defects occur in the outflow tract of the heart, with absence of septation of the conotruncus below the valve level and interrupted aortic arch, a phenotype known in humans as persistent truncus arteriosus (type A4). In addition, semilunar valves do not form in mutants, while the atrioventricular valves appear unaffected. Abnormal septation of the heart and valve anomalies are the most frequent forms of congenital cardiac defects in humans; however, most mouse models display broad defects throughout cardiac tissues. The more restricted spectrum of cardiac anomalies in *Bmpr2*$^{\Delta E2}$ mutants makes this strain a key murine model to understand the embryonic defects of persistent truncus arteriosus and impaired semilunar valve formation in humans.

Key words: Bone morphogenetic protein, Endocardial cushion, Outflow tract septation, Persistent truncus arteriosus, Hypomorph, Semilunar valve

INTRODUCTION

Bone morphogenetic proteins (BMPs) constitute the largest group of the transforming growth factor β (TGFβ) superfamily of growth factors, and are involved in a wide variety of inductive processes during embryonic development, as well as in maintenance of adult tissues (reviewed by Hogan, 1996). The large number of BMPs, their overlapping patterns of expression in many tissues, and the relatively mild phenotypes of several mouse models deficient for widely expressed BMPs, raise the issue of functional redundancy (Lyons et al., 1995; Storm and Kingsley, 1996; Solloway et al., 1998). BMPs signal through heteromeric complexes of two types of transmembrane serine threonine kinase receptors, I and II (Liu et al., 1995). As few receptors have been identified in proportion to the number of BMP ligands, a major question has been to understand how specificity of BMP action is achieved. One aspect of specificity is thought to be the differential affinities of the ligands for one of three type I receptors: ActRI (Acvr1), Bmpr1a and Bmpr1b (ten Dijke et al., 1994; Chen et al., 1998; Macías-Silva et al., 1998). So far only two type II receptors that can transduce BMP signals in vitro have been identified, Bmpr2 (Liu et al., 1995; Nohno et al., 1995; Rosenzweig et al., 1995) and ActRII (Acvr2), originally identified as a receptor for activins (Yamashita et al., 1995; Piek et al., 1999). The majority of *Acvr2*$^{-/-}$ mice die at birth due to palatal defects, but 20% live to be infertile adults (Matzuk et al., 1995a). The extent to which these phenotypes reflect impaired signaling through the activin versus BMP pathways is not known. *Bmpr2* null mouse mutants die in utero at gastrulation (Beppu et al., 2000), demonstrating that Bmpr2 is required for primitive streak formation. The early embryonic lethality associated with loss

of Bmpr2 function precludes an analysis of the role of this receptor at later stages of development. Therefore, the generation of an allelic series consisting of impaired function alleles is needed in order to identify morphogenetic events that are sensitive to reduced levels of BMP signaling at later stages.

The potential importance of gene dosage in BMP signaling is highlighted by the recent finding that, in humans, mutations in the *BMPR2* gene, thought to lead to haploinsufficiency, cause primary pulmonary hypertension (PPH), a vascular disease that is caused by increased proliferation of endothelial and smooth muscle cells in the pulmonary arteries (Deng et al., 2000; Lane et al., 2000). We report the generation of mice carrying a modified allele of *Bmpr2*, *Bmpr2*$^{\Delta E2}$, which encodes a protein that lacks half of the extracellular ligand-binding domain. Mice homozygous for this mutant allele display a mild skeletal phenotype, which includes posterior transformation of the last thoracic vertebra, consistent with a reduction of BMP signaling in these mutants. The mutants die before birth with cardiovascular defects. As opposed to most mouse models of congenital cardiac defects, *Bmpr2*$^{\Delta E2}$ mutants have a fully penetrant, very restricted phenotype, which is limited to the outflow tract. The defect associates an absence of septation of the outflow tract of the heart with interruption of the aortic arch, a condition known in humans as persistent truncus arteriosus type A4 (Jacobs, 2000). In addition, the semilunar valves, which prevent backflow from the aorta and pulmonary trunk into the ventricles, do not form in mutants. The signaling pathways responsible for the differentiation of the conotruncal ridges into both the conotruncal septum and the semilunar valves are very poorly understood. We show that an intact BMP signaling pathway is required for maintenance of the conotruncal ridges and formation of the semilunar valves.

MATERIALS AND METHODS

Generation of *Bmpr2*$^{\Delta E2}$ mice

Bmpr2 clones were isolated from a 129/SvJ mouse genomic DNA BAC library (Incyte). A 13 kb *Bam*HI fragment containing exons 2 and 3 subcloned into pBluescript II KS (Stratagene) was used to build the targeting construct. The construct was generated by replacing a 2.2 kb *Bgl*II fragment containing exon 2 with a PGKneopA cassette. The 5′ flank consists of a 6 kb *Eco*RI/*Bgl*II cassette, and the 3′ flank consists of a 2.5 kb *Bgl*II/*Aat*II fragment. An MC1-thymidine kinase cassette (MC1tkpA) was placed on the 5′ end of the construct. The construct was linearized by digestion with *Sal*I, and electroporated into RW4 ES cells (Incyte) according to established protocols (Ramirez-Solis et al., 1993). Targeted clones were injected into blastocysts by the UCLA Transgenic Mouse Facility. Chimeric mice were mated with Balb/cJ females, and albino and chinchilla offspring were analyzed by Southern blot hybridization. Chimeras were also bred to C57Bl/6J females. Phenotypic analyses were performed on embryos with mixed Balb/cJ × 129SvJ or mixed C57Bl/6J × 129SvJ backgrounds. No differences in the cardiac phenotype were noted for the different genetic backgrounds. *Bmpr2*$^{\Delta E2}$ mice were identified using a 600 bp 5′ external probe by Southern blot analysis of *Bam*HI/*Xho*I-digested DNA prepared by tail biopsy. This strategy distinguishes a 14 kb wild-type allele from the 8 kb targeted allele (not shown). Subsequent genotyping was performed using a ~350 bp internal probe encompassing exon 3 to distinguish between a 5 kb wild-type allele from the ~1 kb targeted allele after digestion of the genomic DNA with *Eco*RV (Fig. 1B). The targeted allele is designated as *Bmpr2*$^{\Delta E2tm1KML}$ according to the guidelines of the International Committee on Standardized Genetic Nomenclature for Mice (The Jackson Laboratory, Bar Harbor, ME) and was abbreviated to *Bmpr2*$^{\Delta E2}$ in this text.

RT-PCR

Total RNA was prepared from E12.5 embryos of each genotype using Trizol (Gibco-BRL) according to the manufacturer's protocol. Reverse transcription was carried out with a gene-specific primer located in exon 5 (E5R, 5′-GTG AAG ACC CTG TTT CCG GTC-3′) with the ProStar kit (Stratagene). A region encompassing exon 2 was amplified by PCR with oligonucleotides E1F (5′-CTT CTT TGC TGG CCC AGG GA-3′) and E3R (5′-TGG TGT TGT GTC AGG GGG TG-3′) or E5R. As a control, a region downstream of the deletion was amplified with primers in exons 3 and 5 (E3F, 5′-GGT CTC ACA TCG GTG ATC CC-3′; E5R as above). Semi-quantitative PCR on cDNA obtained from wild-type, mutant and heterozygous littermates was performed with oligonucleotides E1F and E5R, by collecting aliquots of each reaction after 12, 18, 22, 25, 28 and 30 cycles, run on gel, imaged, scanned and quantified. No differences in levels of expression of *Bmpr2* and *Bmpr2*$^{\Delta E2}$ were observed.

Generation of *Bmpr2* and *Bmpr2*$^{\Delta E2}$ expression constructs and transfections

cDNA was prepared from the above-described total RNA using Superscript II reverse transcriptase and random hexamers (Gibco-BRL). Full-length coding sequences for *Bmpr2* and *Bmpr2ΔE2* were obtained by PCR using the *Bmpr2*$^{+/+}$ and *Bmpr2*$^{\Delta E2/\Delta E2}$ cDNAs, respectively, as templates, and the following primers: 5′-ctgaattc TTC TTT GCT GGC CCA GGG ATG AC-3′ and 5′-tgtctaga AAC ATC TCA CAG ACA ATT CAT TC-3′ [lowercase letters indicate nucleotides added to the sequence (e.g. to include restriction sites) that do not match the sequence of the gene to be amplified]. The resulting amplification products were digested with *Eco*RI and *Xba*I, and subcloned into pBluescript II KS (Stratagene). The subclones were sequenced on both strands to verify that no mutations were introduced. The sequence analysis also verified that exon 2 is absent from the gene product of the mutant allele. The *Eco*RI/*Xba*I fragments encoding *Bmpr2* and *Bmpr2ΔE2* were introduced into pcDNA3 (Invitrogen) to generate pcDNA-Bmpr2 and pcDNA-Bmpr2ΔE2.

Mv1Lu or P19 cells (ATCC) at 50-70% confluence were transfected, using the Superfect transfection reagent (Qiagen), with 0.5 μg of *msx2*-Lux (Liu et al., 1994; Daluiski et al., 2001), 0.5 μg of *lacZ*-encoding control plasmid and 0.05 μg of either pcDNA-Bmpr2 or pcDNA-Bmpr2ΔE2 per well. After 3 hours, medium was replaced by MEM + 1% FBS + non essential amino acids. Twenty-four hours post-transfection, recombinant human BMP2 or BMP7 (Genetics Institute) was added where indicated. After an additional 24 hours, cells were lysed with Reporter lysis buffer (Promega) and luciferase activity measured with the Luciferase Assay System (Promega). Results were obtained in triplicate for each experiment and normalized to β-galactosidase activity. The results shown in Fig. 1F are normalized for four and two independent experiments for BMP2 and BMP7, respectively. Statistical significance was assessed using a *t*-test for correlated samples using the Vassar website (http://faculty.vassar.edu/lowry/VassarStats.html).

Ink injection

India ink was injected into the ventricles of the hearts of two litters of E12.5 and three litters of E13.5 embryos with custom-made pulled glass pipettes and an Eppendorf micro-injector. Each embryo was genotyped a posteriori with genomic DNA made from its yolk sac. Ink was allowed to circulate, and embryos were fixed into 4% paraformaldehyde (PFA) overnight, dehydrated in an increasing series of methanol and cleared in benzyl benzoate:benzyl alcohol (2:1).

Cleared skeletal preparation, histology and in situ hybridization

Cleared skeletal preparations were performed as described (Hogan et

al., 1994). Embryos were fixed in 4% PFA and embedded in paraffin wax, sectioned (7 μm) and stained with Eosin/Hematoxylin according to standard techniques. TUNEL analysis was performed on 7 μM paraffin wax-embedded sections with Promega's Apoptosis Detection System according to the manufacturer's instructions. Cell proliferation was assessed by immunohistochemistry with antibodies against the Proliferating Cell Nuclear Antigen (PCNA, Zymed). Immunohistology for smooth muscle actin was performed with the monoclonal anti-αSMA clone 1A4 (Sigma). Whole-mount in situ hybridization was performed as described (Hogan et al., 1994), with BM Purple (Boehringer Mannheim) as a substrate for alkaline phosphatase. For in situ hybridization on sections, the embryos were embedded into OCT medium (VWR), and 20 μm cryosections were cut and processed as described (Hogan et al., 1994). The *Bmp4* probe was as described (Jones et al., 1991). The *Pax3* probe is a gift from Dr P. Gruss. The probe for *Ctgf* was made from IMAGE clone dbEST #723742. The periostin and *Tbx1* probes were cloned by RT-PCR using whole-embryo RNA as described previously (Kruzynska-Frejtag et al., 2001; Garg et al., 2001).

RESULTS

Construction of a hypomorphic allele of Bmpr2

We generated mice lacking exon 2 of the *Bmpr2* gene (Fig. 1A,B). The 171 nucleotides of exon 2 code for half of the extracellular ligand-binding domain of Bmpr2 (Beppu et al., 1997). This includes three of seven cysteine residues, conserved among all type II receptors, that are required to maintain the conformation of the extracellular domain, and two of five hydrophobic amino acids thought to participate in the hydrophobic interactions that stabilize the structure (Fig. 1C) (Greenwald et al., 1999; Guimond et al., 1999).

Since the first four exons of *Bmpr2* are in frame, we hypothesized that deleting exon 2 would maintain the reading frame and produce a shorter, but correctly translated, protein (Fig. 1D). To verify this, we performed RT-PCR using RNA extracted from wild type, heterozygous and homozygous mutant embryos. For all genotypes, an amplified product was obtained with primers downstream of the mutation (between exons 3 and 5), as well as with primers spanning the deletion, indicating that a stable mRNA is transcribed from the mutant allele (Fig. 1E). Semi-quantitative PCR confirmed that the levels of expression of the wild-type and mutant alleles are not significantly different (not shown). The difference in size

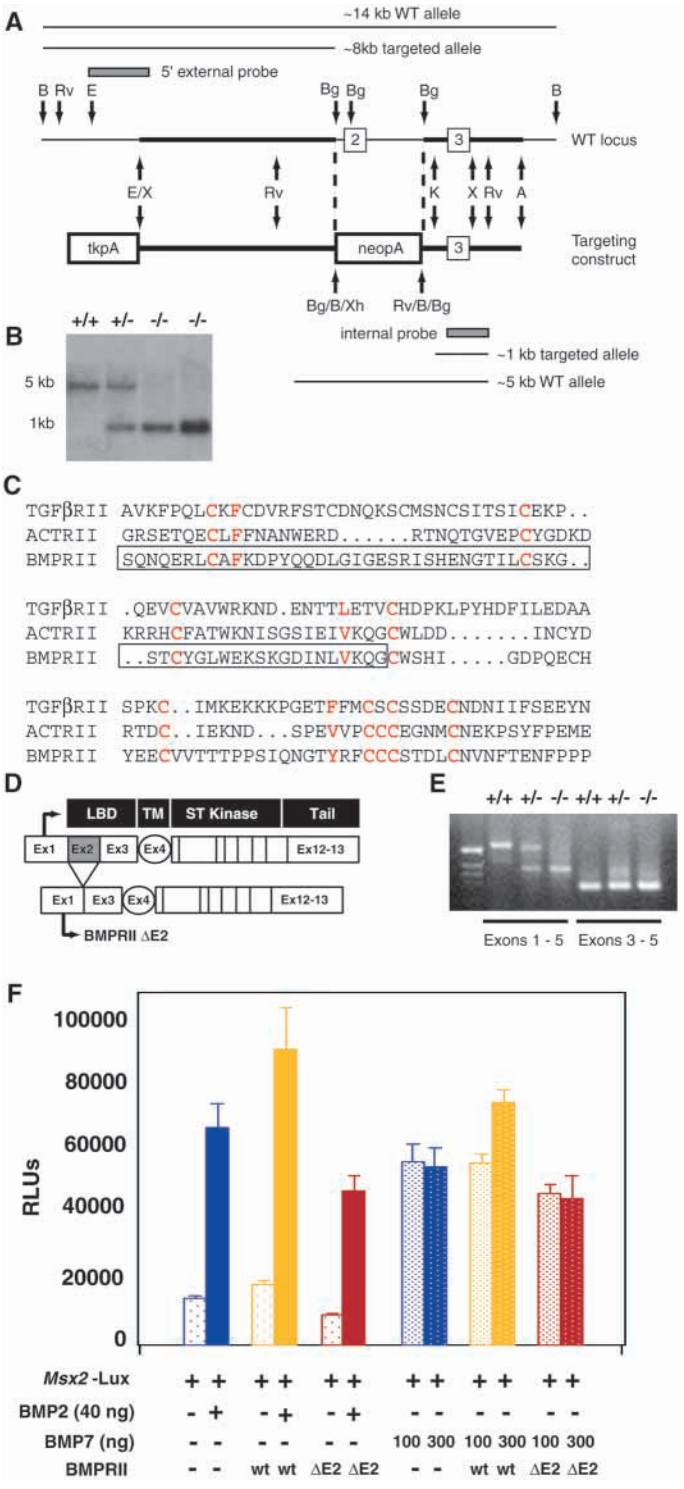

Fig. 1. A functional truncated protein is encoded by the *Bmpr2*$^{\Delta E2}$ allele. (A) Targeting strategy. Exon 2 of *Bmpr2* was replaced by a neomycin resistance cassette. A, *Aat*II; B, *Bam*HI; Bg, *Bgl*II; E, *Eco*RI; Rv, *Eco*RV; K, *Kpn*I; X, *Xba*I; Xh, *Xho*I. (B) Southern blot showing genotyping of pups with the internal probe. (C) Amino acid sequence comparison of the extracellular domains of mouse ActRII, TGFβRII and Bmpr2. The region encoded by exon 2 is boxed and conserved residues involved in 3D-structure formation are in red. This includes three out of seven cysteine residues, which are conserved among all type II receptors, that are required to maintain the conformation of the extracellular domain, and two out of five hydrophobic amino acids thought to participate in the hydrophobic interactions that stabilize the structure. (D) Structure of the Bmpr2 protein. Exon 1 encodes the initiator methionine. Exons 2 and 3 each encode half of the extracellular ligand-binding domain. Exon 4 encodes the transmembrane domain. The serine threonine kinase domain is encoded by exons 5-11. Exons 12-13 encode an intracytoplasmic tail of unknown function. Deletion of exon 2, which is in frame, should generate a truncated protein. (E) RT-PCR on RNA from wild type (+/+), heterozygous (+/–) and ΔE2 mutants (–/–) with primers encompassing the deletion (exons 1-5) and downstream of the deletion (exons 3-5) shows that the *Bmpr2*$^{\Delta E2}$ allele is transcribed. (F) Transfection of the mutant or wild-type Bmpr2 cDNA expression plasmid confers BMP responsiveness to Mv1Lu cells. BMP signaling activity was assayed with a reporter construct that contains luciferase under the control of a BMP-responsive element from the promoter of the *Msx2* gene (Daluiski et al., 2001; Liu et al., 1994).

between the mutant and wild-type PCR products corresponded to the size of exon 2. Cloning and sequencing of the full-length wild-type and *Bmpr2*$^{\Delta E2}$ cDNAs confirmed that exon 2 was deleted and that exons 1 and 3 were in frame in the mutant.

Responsiveness to BMPs of cells transfected with the mutant *Bmpr2*$^{\Delta E2}$ cDNA was assayed with a reporter construct that contains luciferase under the control of a BMP-responsive element from the promoter of the *Msx2* gene (Liu et al., 1994; Daluiski et al., 2001). Addition of BMP2 to Mv1Lu cells led to a three- to fourfold stimulation of the BMP pathways (Fig. 1F, columns 1 and 2). Transfection with the wild-type receptor increased the level of induction to approx. fivefold (Fig. 1F, columns 3 and 4). However, in cells transfected with the Bmpr2$^{\Delta E2}$ receptor, a significantly lower induction was observed (columns 5 and 6; $P<0.025$), showing that BMP signaling is reduced in the presence of the mutant receptor. Similar results were obtained when transfecting P19 cells under the same experimental conditions (data not shown).

BMP7, a ligand of a different subclass, was also able to induce luciferase expression in Mv1Lu cells, albeit with less efficacy (Fig. 1F, columns 1, 9 and 10). Transfection with Bmpr2 did not lead to increased *msx2*-Lux induction in response to 100 ng/ml BMP7 (Fig. 1F, columns 7 and 9), but a 1.4-fold increase was observed in response to 300 ng/ml BMP7 (Fig. 1F, columns 8 and 10). By contrast, cells transfected with Bmpr2$^{\Delta E2}$ were unresponsive to BMP7 at either concentration (Fig. 1F, columns 11 and 12).

These results indicate that Bmpr2$^{\Delta E2}$ has reduced signaling capacity compared with wild type Bmpr2. The stability, ligand binding and signal transduction properties of the mutant receptor that contribute to the defective signaling properties will be described in detail elsewhere. The diminished signaling capacity of cells overexpressing the mutant receptor compared with control cells (Fig. 1F, columns 2, 4 and 6) suggests that either Bmpr2$^{\Delta E2}$ has dominant-negative properties, or that overexpression of this altered receptor leads to sequestration of BMP ligands and/or type I receptors into impaired signaling complexes. In fact, this apparent dominant negative effect in vitro when overexpressed has been observed for other *Bmpr2* mutant receptors which do not have such effects in vivo, and is thought to be an artifact due to interference with intracellular trafficking in transfected cells (Rudarakanchana et al., 2002). The observations that heterozygotes exhibit no apparent defects, and that the phenotype of *Bmpr2*$^{\Delta E2/\Delta E2}$ mutants (see below) is much less severe than that of mice homozygous for the *Bmpr2* null allele (Beppu et al., 2000), strongly argue that *Bmpr2*$^{\Delta E2}$ is not a dominant-negative or null allele but retains some signaling capacity and thus is a hypomorphic allele.

Viability of the *Bmpr2*$^{\Delta E2/\Delta E2}$ mutants

Heterozygous males and females were viable and fertile, with no apparent malformations. Intercrosses of heterozygotes produced no live homozygous mutants, indicating an embryonic lethal phenotype. Up to E11.5, mutants were found in expected Mendelian ratios (39 *Bmpr2*$^{\Delta E2/\Delta E2}$ out of 154 embryos at E11.5). Up to this stage, mutants are alive and phenotypically indistinguishable from wild-type or heterozygous siblings (not shown). Dissection of litters at later gestational ages showed that, even within the same litter, mutants die at various stages (Fig. 2A-C), with the onset of lethality occurring between E12 and birth. Anomalies of vascularization of the yolk sac, consisting of regions without apparent vessels, were noted upon dissection (not shown). The avascular regions were larger for embryos that had died before E12.5 than for embryos that died at later stages, suggesting that yolk sac vascular anomalies could represent a major contribution to the early lethality of the mutants. This aspect of the phenotype will be reported elsewhere.

Skeletal phenotype of *Bmpr2*$^{\Delta E2/\Delta E2}$ mutants

BMP signaling pathways are essential for skeletal patterning and growth (Hogan, 1996), and Bmpr2 is thought to be the common receptor for all osteogenic BMPs. Therefore, the observation of a skeletal phenotype is predicted in animals with decreased BMP signaling through Bmpr2$^{\Delta E2}$.

Whole-mount cleared skeletal preparations of whole litters aged E14.5-E18.5 confirmed that ossification was delayed in mutants compared with their siblings. This was observed in both endochondral and membranous bones. It was particularly severe in the lateral ossification centers of cervical vertebrae C3-C6, the fourth sternebra (not shown), the ventral processes of cervical vertebrae C1-C4 and the interparietal bone (Fig. 2D,E). Whether this results from a general developmental delay or from a specific defect of osteogenesis is not immediately apparent. Although there was no overt growth

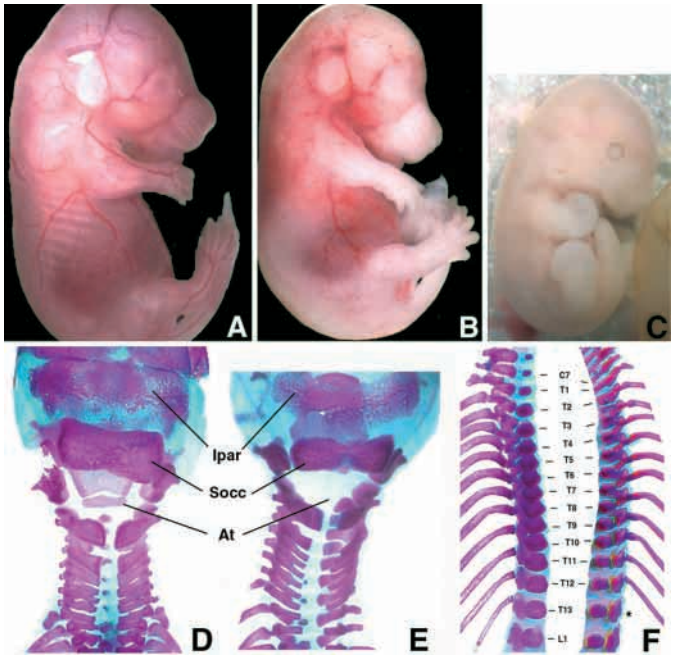

Fig. 2. Skeletal phenotype of *Bmpr2*$^{\Delta E2/\Delta E2}$ mutants. (A-C) Three siblings from a litter dissected at E15.5 showing that mutants die at various stages of gestation. (A) wild type (WT), (B) mutant dead at E14.5, (C) mutant dead at E12, as judged by the extent of limb development. (D-F) Cleared skeletal preparations of two siblings, recovered dead at birth. Dorsal views of the base of the skulls of WT (D) and mutant (E) illustrate the major ossification delay of the interparietal bone (Ipar), and of the ventral processes of the cervical vertebrae 1-4, in particular of the atlas (At). Socc, supraoccipital bone. (F) Ventral views of the half vertebral columns of wild type (left) and mutant (right) showing the absence of the thirteenth rib in the mutant (asterisk). Thoracic (T1-T13) and lumbar (L1) vertebrae are numbered. Note the ossification delay of the ventral and lateral ossification processes of the vertebrae in the mutant.

defect, a vascular defect could conceivably result in developmental delay of the *Bmpr2*$^{\Delta E2}$ mutants. However, the observation that specific skeletal elements (e.g. atlas) are more severely affected than others argues for a primary defect in skeletogenesis.

Loss of the 13th pair of ribs, associated with a posterior transformation of the 13th thoracic vertebra into a 7th lumbar vertebra, was observed in all the mutants, independent of the genetic background (n=9 homozygotes, Fig. 2F). Therefore, in addition to a role in skeletal growth, full activity of Bmpr2 is essential for skeletal patterning along the anteroposterior axis.

Cardiac septation defects in *Bmpr2*$^{\Delta E2/\Delta E2}$ mutants

The onset of lethality over several days at late gestation stages suggested a cardiovascular defect. The external aspect of the heart was normal in mutants up to E12 (not shown). At later stages, two normally septated vessels, the aorta and the pulmonary trunk were seen exiting the arterial pole of the heart, but their abnormal relative position was noted (Fig. 3A,B). Closer inspection suggested that although the outflow tract was septated distally into aorta and pulmonary trunk, the region proximal to the heart was not septated. Moreover, a dimple at the apex of the ventricle, a common sign of incomplete ventricular septation, was noted in mutants (Fig. 3B).

To help visualize the anatomy of the outflow tract, we injected ink into the ventricles of embryos. At E13.5, when septation of the ventricle into a left and a right cavity is complete in wild-type embryos, injection of ink into the right ventricle of mutants immediately resulted in leakage of ink into the left ventricle, confirming a ventricular septal defect. The ink injections also documented abnormal septation of the proximal part of the outflow tract (OFT) of the heart, the conotruncus, with a single lumen and no separation between right and left vessels (Fig. 3D). Histological examination revealed that the ventricular septal defect observed in mutants is not due to a simple developmental delay, because it is observed at all stages of gestation (e.g. Fig. 4D,I-J). Histological examination at E14.5 and E16.5 also confirmed that OFT septation is abnormal. Massive absence of the conal cushions (Fig. 4J,K) was visible as early as E12.5, although one of the posterior conal cushions was present (arrowhead in Fig. 4D,K) in mutants.

Interrupted aortic arch in *Bmpr2*$^{\Delta E2/\Delta E2}$ mutants

In addition to abnormal septation of the conotruncus and a ventricular septal defect, ink staining also revealed interruption of the aortic arch (Fig. 3E-G), of varying severity, between the roots of the left common carotid and the left subclavian artery (IAA type B), resulting in extensive communication between the pulmonary trunk and the descending aorta, via the ductus

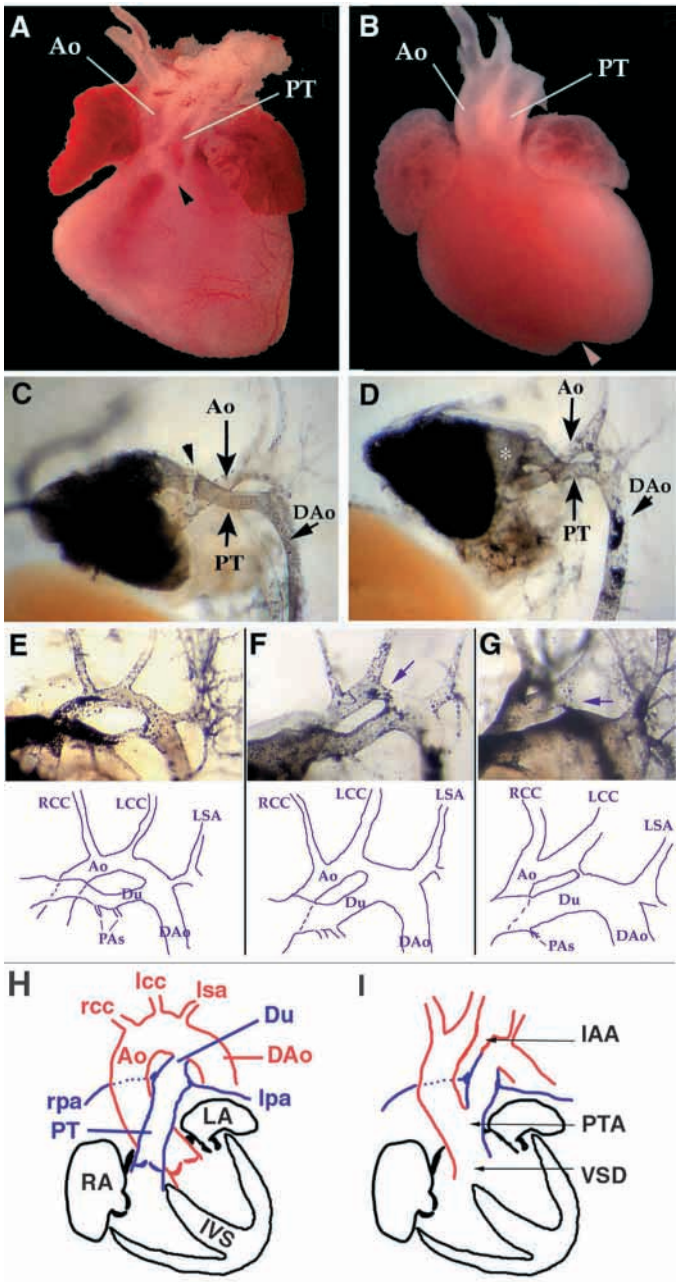

Fig. 3. External aspect of the hearts of *Bmpr2*$^{\Delta E2/\Delta E2}$ mutants. (A,B) Frontal views of wild-type (A) and *Bmpr2*$^{\Delta E2/\Delta E2}$ mutant (B) hearts at E16 showing a normally septated ascending arch of the aorta (Ao) and pulmonary trunk (PT) distally, but not proximally to the heart. The black arrowhead in A indicates the semilunar valves of the PT. The pink arrowhead in B indicates a dimple at the apex of the ventricle, a common sign of ventricular septal defect. (C-G) Ink-injected E13.5 hearts. Left lateral views of whole-mount India ink-injected wild-type (C) and *Bmpr2*$^{\Delta E2/\Delta E2}$ (D) hearts. The arrowhead in C indicates the semilunar valve level. Semilunar valves are absent in mutants. The white asterisk in D indicates the non-septated conotruncus of the mutants. DAo, descending aorta. (E-G) Interruption of the aortic arch (purple arrow) of varying severity in two mutants (F,G) is visible between the left common carotid artery (LCC) and the left subclavian artery (LSA) in the ink-injected outflow tract (upper panel) and derived cartoons (lower panels). The ductus arteriosus (Du) is enlarged. Pulmonary arteries (PAs) stem normally off of the pulmonary trunk in the mutants. RCC: right common carotid artery. (H,I) Cartoon of a WT (H) and *Bmpr2*$^{\Delta E2/\Delta E2}$ mutant (I) heart showing the association of persistent truncus arteriosus (PTA), ventricular septal defect (VSD) and interrupted aortic arch type B (IAA) that constitute the type A4 persistent truncus arteriosus (Jacobs, 2000). Ao, aorta; DAo, descending aorta; Du, ductus arteriosus; IVS, interventricular septum; LA and RA, left and right atria, respectively; LCC and RCC, left and right common carotids, respectively; LPA and RPA, left and right pulmonary arteries, respectively; LSA, left subclavian artery; PT, pulmonary trunk.

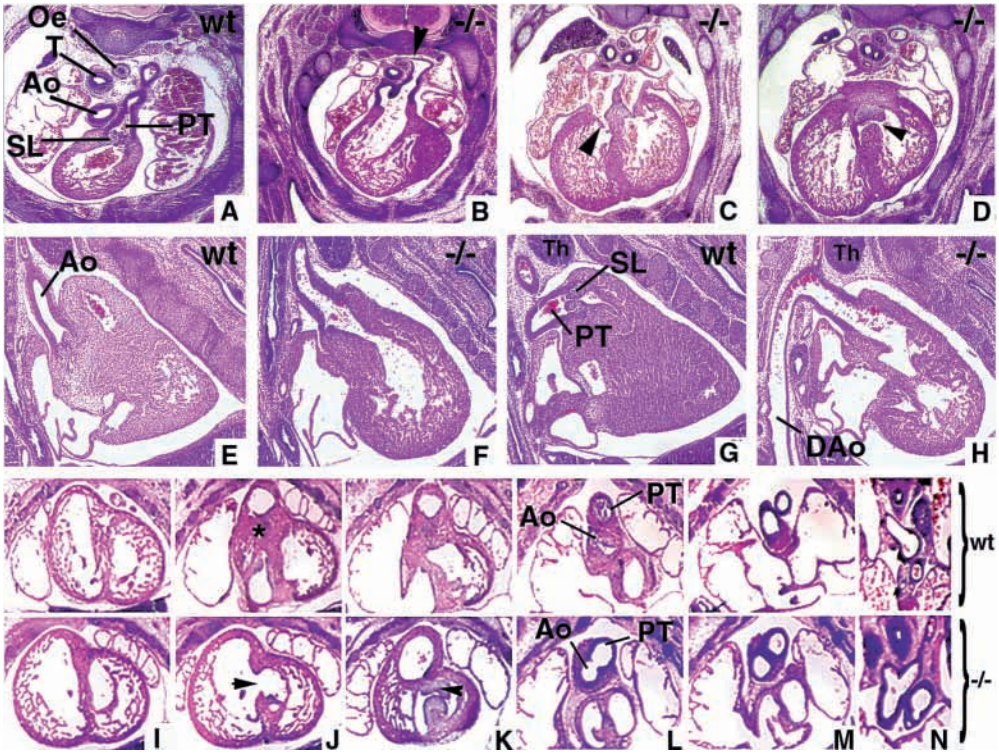

Fig. 4. Histology sections through the hearts at E12.5, E14.5 and E16.5. (A-D) Transverse sections through E14.5 wild-type (A) and *Bmpr2*$^{\Delta E2/\Delta E2}$ (B-D) hearts show a common origin to the aorta (Ao) and pulmonary trunk (PT) and total absence of semilunar (SL) valves (B), while the valves of the atrioventricular canal develop normally (arrowhead in C). A ventricular septal defect is associated (arrowhead in D). The left subclavian artery was occasionally retro-esophageal (arrowhead in B). Oe, Esophagus. T, Trachea. (E-H) Sagittal sections through E16.5 wild-type (E,G) and mutant (F,H) hearts show the aorta (E,F) and the pulmonary trunk (G,H) exiting the same ventricle in the mutants. The pulmonary trunk is the main vessel connecting to the descending aorta (DAo), as a result of the hypoplasia of the aortic isthmus. Note that the thymus (Th) is of normal size in the mutant. (I-N) Series of frontal sections (dorsal to ventral) of an E12.5 wild-type (top panels) and a mutant (lower panels) heart show that, posteriorly, ventricular septation is normal (I), but at the base of the pulmonary trunk, a large ventricular septal defect is visible (black arrow in J). One of the conal cushions appears to form correctly (arrowhead in mutant, K) but most conal tissue (asterisk in wild type, J) is already missing (K). The outflow tract starts septating into two arteries at about the same level that the semilunar valves form in the wild type (L), and aorta and pulmonary trunk are fully septated and in normal relative position beyond that point (M). The aorta branches into the right subclavian artery, while the pulmonary arteries (PAs) arise normally from the pulmonary trunk (N).

arteriosus. This regression of the aortic isthmus (which derives from the left aortic arch 4) was also observed histologically (Fig. 4H). The varying severity observed at early stages reflects a progressive regression occurring at these stages of intense remodeling of the aortic arches. The interruption of the aortic arch was complete (and fully penetrant) in animals observed at later gestation stages.

Except for occasional retro-esophageal position of the left subclavian artery (Fig. 4B), the development of neighboring tissues was normal. The pulmonary arteries stemmed normally from the pulmonary trunk (Fig. 3F,G, Fig. 4N). In particular, other tissues affected in neural crest deficiency syndromes were unaffected: thymus (Fig. 4G,H) and thyroid (not shown) were present and no tracheo-esophageal fistula was observed (Fig. 4B).

The semilunar valves are absent in *Bmpr2*$^{\Delta E2/\Delta E2}$ mutants

Semilunar valves prevent backflow of the blood from the aortic and pulmonary trunks into the ventricles. They form at the junction of the conotruncus and the aortic sac, hypothetically by remodeling of the top part of the conotruncal ridges. No evidence for the presence of semilunar valves was detected in the outflow tract of ink-injected mutant hearts (Fig. 3C,D). Histology at various gestational stages demonstrated that semilunar valve tissue is completely absent in mutants after E12.5 (Fig. 4A-B,E-H,L). The defect was limited to the outflow tract, and the atrioventricular (future mitral and tricuspid) valves were grossly normal (Fig. 4C).

Absent septation of the OFT results from impaired growth of the conotruncal ridges

Two major cell types contribute to the formation of the conotruncal swellings that eventually fuse to septate the outflow tract: the endocardium and the neural crest.

Starting around day E9.5 in the mouse, the resident endocardium, under the influence of inductive signals from the underlying myocardium, undergoes an epithelio-mesenchymal transformation (EMT), which can be followed by histological analysis. At E11.5, the swellings are of maximum thickness in wild-type mice and fill the entire lumen of the outflow tract (Fig. 5A,C). In the mutants, the EMT has occurred, and ridges have started to form (Fig. 5B,D), suggesting that intact BMP signaling is not required for induction of the EMT. However,

in mutants, the swellings are much thinner than in wild type, and cell density is lower (see the zones of cell-free cardiac jelly in Fig. 5B,D). No increase of cell death was observed by TUNEL analysis (not shown). However, by E12.5, the swellings are no longer apparent (Fig. 4K), suggesting that BMP signaling is involved in the continued development and/or maintenance of the conotruncal cushion tissue.

Cell proliferation rates in OFT cushions vary widely with the cell type, the stage of differentiation, and the position of the cells within the cushion (Kubalak et al., 2002). Therefore, the very different shapes and sizes of the cushions in mutants compared with wild-type embryos do not allow direct comparison of proliferation rates of each region. However, PCNA staining in myocardial cells was indistinguishable in wild-type and mutant littermates (Fig. 5E-G). Abundant PCNA-positive cells were found both in wild-type and mutant cushions, showing that, despite the reduced size of the cushions at E11.5, mesenchymal cells proliferate extensively in the mutant (Fig. 5E-G). However, as the two sections from the same mutant embryo illustrate (Fig. 5F-G), high variability was found in the extent of cell proliferation in different regions of the mutant OFT cushions, which could reflect abnormal growth regulation of these cells. This high variability in cell proliferation has also been noted within cushions of *Bmp6*$^{-/-}$;*Bmp7*$^{-/-}$ mice (Kim et al., 2001).

Neural crest cells originating from the posterior rhombencephalon migrate through pharyngeal arches 3, 4 and 6, and contribute to the swellings (Kirby, 1999; Jiang et al., 2000). An essential role for cardiac neural crest cells in septation of the mammalian outflow tract has been inferred from studies of various mutant mouse strains (reviewed by Kirby, 1999), but the role these cells play is unknown. The best studied neural crest deletion syndrome with conotruncal abnormalities is the DiGeorge/Velo-Cardio-Facial spectrum. Most individuals with this condition harbor a large deletion of chromosome 22q11, and the phenotype is thought to be caused by the haploinsufficiency of the genes located in this region. Among the deleted genes, *TBX1* is the main candidate for the

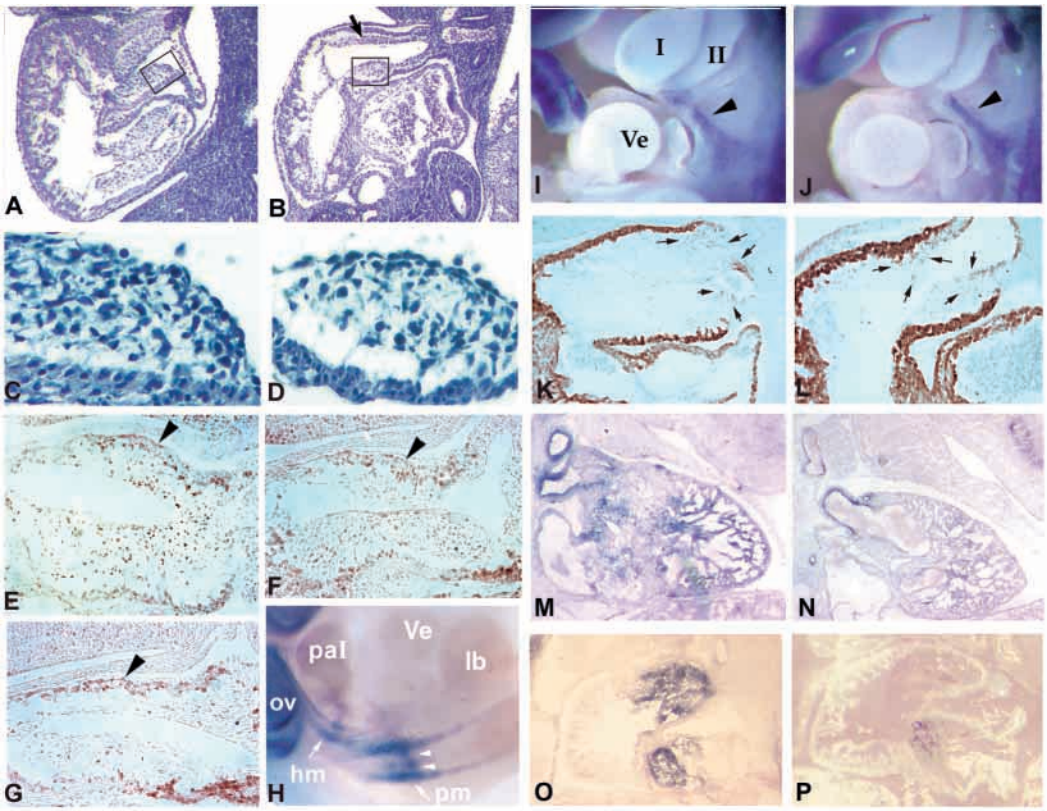

Fig. 5. Impaired OFT cushion growth in *Bmpr2*$^{\Delta E2/\Delta E2}$ mutants. (A-D) Sagittal sections at E11.5 show that the conotruncal ridges (arrow) form in the mutant (B), but not to the extent that they do in the wild type (A). (C,D) Higher magnifications of the boxed areas in A,B, respectively. (E-G) Immunostaining for PCNA in OFT cushions of E11.5 wild type (E) and a mutant (F,G) littermate. The arrowheads indicate the myocardium. (H) *Tbx1* expression at E10.5 in a *Bmpr2*$^{\Delta E2/\Delta E2}$ mutant is found in the posterior part of the otic vesicle (ov), head mesenchyme (hm) and the mesenchyme surrounding the paired dorsal aortae (pm), as well as the dorsal wall of the aortic sac, with higher intensity in the posterior-most region (arrowheads) as described in wild type (Garg et al., 2001; Merscher et al., 2001; Vitelli et al., 2002). Anterior is towards the left and ventral towards the top. paI, pharyngeal arch I; Ve, ventricle; lb, left anterior limb bud. (I,J) *Pax3* expression in neural crest cells (arrowhead) migrating in the neck region at E10.5 was normal in mutants (I, wild type; J, mutant). Pharyngeal arches are numbered in Roman numerals. Ve, ventricle. (K,L) Smooth muscle actin-positive neural crest cells (arrows) reach the outflow tract endocardial ridges in both the wild type (K) and mutant (L) E11.5 embryos. (M,N) At E13.5, in wild type embryos, *Ctgf* expression was detected in the pulmonary trunk and aorta, predominantly in the cell layers closer to the lumen, as well as in a punctate pattern in the ventricles (M). Myocardial expression is predominantly in the trabecular zone of the ventricles. Expression was not modified in mutants (N). (O,P) The expression of periostin, a BMP-regulated gene, was downregulated in the endocardial ridges of E11.5 mutants (P) compared with wild-type littermates (O). To help visualize the tissues in absence of background expression, P is an overlay of two different light exposures of the same section.

conotruncal defects observed (reviewed by Botta et al., 2001). In the *Bmpr2*$^{\Delta E2}$ mutants, the levels and sites of expression of *Tbx1* were not affected (Fig. 5H). Pax3 is a transcription factor expressed in neural crest cells, including those that are fated to populate the outflow tract (Jiang et al., 2000). *Pax3*-deficient mice present with generalized neural crest defects including conotruncal abnormalities (Conway et al., 1997). To examine whether the septation defects in mice arise as a consequence of impaired migration of cardiac neural crest, we examined *Pax3* expression. At E10.5, a stream of *Pax3*-expressing neural crest cells is seen migrating toward the OFT (Fig. 5I). These cells are not affected in the *Bmpr2*$^{\Delta E2}$ mutant (Fig. 5J). Although previously thought to be cells fated to the OFT, they are actually migrating toward the hypoglossal muscle (Epstein et al., 2000). In addition, smooth muscle actin (SMA)-positive cells, which represent at least a subset of the cardiac neural crest (Epstein et al., 2000), were found to reach the outflow tract in mutant as in wild-type embryos (Fig. 5K,L). These results, showing that *Tbx1, Pax3* and SMA expression is unaffected, along with the absence of defects in other neural crest-derived tissues argue against a general defect in neural crest migration. However, an effect of BMP signaling on survival and/or differentiation of neural crest cells within the outflow tract is possible.

The expression of genes implicated in EMT was examined to determine whether this process is impaired in mutants. *Bmp2* and *Bmp4* are expressed in the myocardium underlying the cushion-forming regions and have therefore been considered candidates for an EMT-inductive myocardial signal (Lyons and Hogan, 1993). *Bmp4* expression was not modified in the *Bmpr2*$^{\Delta E2}$ mutants (data not shown). Connective tissue growth factor (*Ctgf*) is an immediate early gene expressed in response to TGFβ treatment (Kothapalli et al., 1997). TGFβs induce EMT in vitro, and are expressed in endocardial cells in regions where cushion formation takes place (reviewed by Nakajima et al., 2000). We found that *Ctgf* was expressed in the conotruncal ridges at day E11.5 (not shown) and in the outflow tract vessels, above the valve level, predominantly in the endothelium (Fig. 5M). Expression of *Ctgf* was not affected in *Bmpr2*$^{\Delta E2}$ mutants (Fig. 5N).

Finally, we tested the expression of periostin, a gene encoding an extracellular matrix protein known to be responsive to BMP signaling in osteoblasts (Ji et al., 2000). Recently, periostin was shown to be expressed at high levels in all cells of the cardiac endocardial cushions (Kruzynska-Frejtag et al., 2001). Periostin expression was greatly diminished in the OFT cushions of *Bmpr2*$^{\Delta E2}$ mutants (Fig. 5O,P), while maintained at high levels in other parts of the embryo, in particular in the ventral mesenchyme (not shown).

DISCUSSION

Different tissues are likely sensitive to different levels of activity of the BMP signaling pathway

BMPs have been shown to elicit dose-dependent effects on patterning during gastrulation (Gurdon and Bourillot, 2001). Levels of BMP signaling are controlled through regulation of the relative concentrations of BMP ligands and antagonists such as noggin and chordin. Activation of TGFβ or activin pathways can also affect BMP signaling activity in vitro via competition for shared signal transduction components (Piek et al., 1999; Candia et al., 1997). In mammals, the identification of developmental events sensitive to reduced BMP signaling has been hampered by the early embryonic lethality or apparent functional redundancy of many mutants deficient in specific BMP ligands or receptors. One approach that has proven successful in overcoming the problem of early lethality has been the generation of conditional knockouts using Cre/loxP technology. A complementary strategy is the generation of alleles with impaired function. These strategies provide different information; the Cre/loxP approach generally tests whether a specific gene product is required in a specific tissue, whereas the generation of altered alleles reveals tissues that are sensitive to changes in levels of gene activity. In this paper, we tested whether a Bmpr2 receptor with reduced function would reveal tissues whose development is sensitive to reduced levels of BMP signaling.

We found that signaling through BMP pathways is reduced in vitro in two different cell lines, with two different classes of BMP ligand, when transfected with the Bmpr2$^{\Delta E2}$ mutant receptor. However, in vitro elucidation of the precise mechanism(s) by which BMP signaling is decreased in the presence of the mutant receptor is hampered by the unavailability of cell lines that do not express endogenous wild-type receptor. This limitation is exemplified in studies of the effects of mutations in individuals with PPH. In this case, the molecular mechanism that lead to disease is thought to be haploinsufficiency of *BMPR2* (Deng et al., 2000; Lane et al., 2000; Thomson et al., 2000; Machado et al., 2001). This conclusion is based on the finding that the altered *BMPR2* alleles in many individuals with PPH encode severely truncated, nonfunctional products. Moreover, some individuals with PPH do not have mutations within the *BMPR2* coding sequence, but nonetheless express *BMPR2* at diminished levels (Atkinson et al., 2002). Although the above findings strongly support haploinsufficiency, an artifactual dominant negative effect, similar to the one we observe, is seen in cell transfection experiments using mis-sense and frameshift *BMPR2* mutations associated with PPH. This effect is most likely to be due to impaired intracellular trafficking, leading to reduced expression of both the mutant and wild-type Bmpr2 at the cell surface (Machado et al., 2001; Rudarakanchana et al., 2002). In addition to the in vitro data, several in vivo observations strongly argue that *Bmpr2*$^{\Delta E2}$ is a hypomorphic allele. *Bmpr2*$^{\Delta E2/\Delta E2}$ embryos survive until midgestation, whereas null mutants die at gastrulation (Beppu et al., 2000). The dramatic difference in severity is not a result of strain-specific differences since we examined mice on several genetic backgrounds, including the 129 strain reported by Beppu and colleagues. These results indicate that Bmpr2$^{\Delta E2}$ retains partial activity in vivo.

The skeletal phenotype also brings strong evidence that BMP signaling is decreased in *Bmpr2*$^{\Delta E2}$ mutants. A general delay in ossification was observed in homozygous mutants, as predicted for a reduced function Bmpr2 allele. No such defects are seen in heterozygotes, arguing against a dominant-negative mode of action. Interestingly, several skeletal elements, such as the supraoccipital bone and ventral process of the atlas, are more affected than others. This result suggests that either different skeletal elements require different levels of BMP signaling for their formation, or that the reduced level of

signaling through the mutant Bmpr2 is compensated in some skeletal elements by another type II receptor.

In addition to defects in bone formation, *Bmpr2*$^{\Delta E2}$ mutants exhibit defects in vertebral patterning. The loss of the 13th thoracic vertebra, and its replacement with a lumbar vertebra, is observed in *Bmpr2*$^{\Delta E2}$ mutants as well as in follistatin-deficient mice (Matzuk et al., 1995b). Follistatin is an activin antagonist. Hence, in *Bmpr2*$^{\Delta E2}$ and follistatin mutants, the level of signaling through activin pathways is expected to be increased relative to the level of BMP signaling. Conversely, GDF11 and ActRIIB are components of activin signaling pathways, and mice deficient in these genes exhibit extra thoracic vertebrae (Oh and Li, 1997; McPherron et al., 1999; Gamer et al., 2001). Along with our results, these findings suggest that regulation of the relative levels of signaling through TGFβ/activin and BMP pathways may play a role in anteroposterior skeletal patterning.

Finally, periostin, a gene that is known to be a downstream target of the BMP pathway in other tissues (Ji et al., 2000), is downregulated in the outflow tract cushions of *Bmpr2*$^{\Delta E2/\Delta E2}$ hearts compared with wild-type and heterozygous littermates. Taken together, the in vitro results, the apparently recessive nature of the *Bmpr2*$^{\Delta E2}$ mutant phenotype, the skeletal phenotypes, and the downregulation of a known target of the BMP pathway are most consistent with a hypomorphic mode of action for Bmpr2$^{\Delta E2}$.

The lethality of homozygotes for a probable null allele of *Bmpr2* around the time of gastrulation (Beppu et al., 2000) is reminiscent of that of null mutants for BMP2 or BMP4 (Winnier et al., 1995; Zhang and Bradley, 1996), suggesting that Bmpr2 is the major receptor for these ligands during gastrulation. The fact that *Bmpr2*$^{\Delta E2/\Delta E2}$ mice undergo normal gastrulation, whereas *Bmpr2* null homozygotes do not, shows that the residual activity of Bmpr2$^{\Delta E2}$ is sufficient to transduce the effects of BMP2 and BMP4 in early development. Similarly, the fact that individuals with PPH with haploinsufficiency of *BMPR2* are viable into adulthood has suggested that 50% of normal BMP pathway activity is sufficient for humans to undergo gastrulation (Deng et al., 2000). Therefore, mesoderm formation during gastrulation does not require full BMP signaling activity. By contrast, the phenotype of the *Bmpr2*$^{\Delta E2}$ mutants shows that morphogenesis of the cardiovascular and skeletal systems does.

Bmpr2$^{\Delta E2}$ mutants: a model for type A4 persistent truncus arteriosus

The cardiovascular phenotype of *Bmpr2*$^{\Delta E2}$ mutants is summarized in the cartoon in Fig. 3H-I. In *Bmpr2*$^{\Delta E2}$ mutants, the distalmost region of the outflow tract is normally septated, suggesting that the wedge of neural crest cells that migrate into the aortic sac to form the aorticopulmonary septum is, at least in part, present. However, the proximal part of the aortic sac and the conotruncus constitute a single outflow vessel, a condition known in humans as persistent truncus arteriosus (PTA) type A1 (as opposed to type A2 where the total length of the outflow tract is non-septated) (Jacobs, 2000).

The absence of the conal cushion tissue, which during normal embryogenesis fuses with the muscular part of the interventricular septum to complete the separation of the ventricles, results in a ventricular septal defect (VSD). Such a membranous VSD is almost always associated with PTA, where it is a hemodynamic necessity (Jacobs, 2000).

In our mutants, the PTA is associated with regression of the aortic isthmus, a tissue that derives from the left aortic arch 4. Such an association of interrupted aortic arch and PTA is also a described entity in humans, known as PTA type A4 (Jacobs, 2000), for which the *Bmpr2*$^{\Delta E2}$ mutants are the first fully penetrant animal model. The form of interrupted aortic arch (Type B), observed in *Bmpr2*$^{\Delta E2}$ mutants, with resorption between the left common carotid and subclavian arteries, is the same as that commonly observed in the DiGeorge/Velo-Cardio-Facial syndromes. However, DiGeorge syndrome is associated with a variable constellation of defects of the heart and neck region and face, including PTA and thymic hypoplasia, that is thought to result from a widespread defect of neural crest cells (Emanuel et al., 1999), a mechanism that is unlikely to cause the phenotype of *Bmpr2*$^{\Delta E2}$ mutants (see below).

Embryological origin of the outflow tract defect: neural crest cells abnormalities or defective epithelio-mesenchymal transformation of the endocardium?

Distally, the single tube that comprises the outflow tract in early midgestation embryos is septated into the aorta and the pulmonary trunk by a structure that is purely neural crest in origin, the aortico-pulmonary septum. This is the structure that is primarily affected in DiGeorge/Velo-Cardio-Facial syndromes, resulting in type A2 PTA.

Proximally, however, septation occurs by a different, less well understood mechanism that requires at least two processes. The first of these is a transformation of endocardial cells into mesenchymal cells that populate the cardiac jelly. BMP signaling may be directly involved in the inductive interactions between myocardium and endocardium during EMT (reviewed by Nakajima et al., 2000). In vitro, BMP2 is not sufficient to trigger the onset of EMT but it can synergize the inductive effect of TGFβs. Consistent with an essential role in vivo, BMP2 and BMP4 expression in the heart is restricted to the regions of myocardium that underlie the cushion-forming regions (Lyons and Hogan, 1993; Nakajima et al., 2000). In *Bmpr2*$^{\Delta E2}$ mutants, we observe initiation of the EMT, but, in the outflow tract, the cushions fail to progress and never reach their maximum extension. This offers genetic evidence that intact BMP signaling is not necessary for initiation of the EMT, but is required for normal growth and maintenance of the conotruncal ridges.

The second process is an invasion of the conotruncal ridges by neural crest cells that may contribute to the cell population forming the septae, and may also be involved in the proliferation and/or survival of the cells that have undergone the EMT. Several studies have shown that BMPs are required in vivo for formation and/or survival of (non-cardiac) neural crest cells (reviewed by Christiansen et al., 2000; Délot et al., 1999). However, the role of cardiac neural crest cells in mammalian endocardial cushion development is poorly understood, and investigations have long been hampered by the absence of consensus molecular markers for the subpopulation of neural crest cells that populate the outflow tract. In particular, the percentage of cells labeled by various proposed neural crest markers is highly variable, and even for a single

marker the extent of labeling varies in different lines of reporter transgenic mice (Brown et al., 2001).

The analysis of splotch (*Pax3*$^{-/-}$) mutants, a mouse model for both total neural crest ablation in chicks and DiGeorge syndrome in humans, has suggested that the bulk number of neural crest cells migrating into the heart is a determining factor for OFT septation (Conway et al., 2000). In *Bmpr2*$^{\Delta E2}$ mutants, neural crest migration, as illustrated by *Pax3* and smooth muscle actin expression, is not massively affected, consistent with defects that are different than in models of total neural crest ablation. In addition to the restriction of PTA to the conus, the adjacent tissues that develop from branchial arches, such as thyroid and thymus, appear normal in *Bmpr2*$^{\Delta E2}$ mutants. Therefore, the aortic arch remodeling defects and OFT septation defect seen in *Bmpr2*$^{\Delta E2}$ mutants are unlikely to result from widespread neural crest ablation. Moreover, cells expressing SMA are present in the OFT of *Bmpr2*$^{\Delta E2}$ mutants, indicating that at least this subset of cardiac neural crest cells migrates to the OFT. Our results are, however, consistent with a role for BMP signaling in cardiac neural crest cells. For example, BMP signaling could be necessary for cell-cell interactions between the newly formed mesenchymal cells arising as a result of EMT and the incoming neural crest cells. The pattern of expression of *Bmpr2* does not offer hints as to which cell type requires intact BMP signaling, as it is ubiquitous throughout the embryo (Roelen et al., 1997) (E. C. D. and K. M. L., unpublished). Fate mapping of the cardiac neural crest (Epstein et al., 2000; Jiang et al., 2000) in *Bmpr2*$^{\Delta E2}$ mutants, as well as tissue-specific targeting of the mutation will therefore be crucial to assess whether subsets of cardiac neural crest cells have different roles in outflow tract septation and valve formation.

Genetic control of valvulogenesis

Semilunar valves develop at the distal end of the conotruncal ridges, hypothetically by remodeling (reviewed by Pexieder, 1995). However, in newborn mice and humans with PTA, although the septum that derives from those ridges is absent, differentiated valves are usually present (albeit with an abnormal number of leaflets). This suggests independent genetic control of septation and valve formation.

Defective semilunar valvulogenesis in *Bmpr2*$^{\Delta E2}$ mutants suggests that the duration and/or strength of BMP signals must be tightly controlled. This is highlighted by the observation of semilunar valve defects in mice deficient in other components of the BMP signaling pathway. Mice deficient for *Tll1*, a mammalian homologue of the *Drosophila* gene *tolloid*, which cleaves the BMP antagonist chordin (Scott et al., 1999), have dysplastic semilunar valves (Clark et al., 1999). Mice mutant for *Smad6*, an inhibitory intracellular mediator of BMP signaling, exhibit hyperplasia of the valves and OFT septation defects (Galvin et al., 2000). The opposing valve phenotypes of *Bmpr2*$^{\Delta E2}$ mutants and *Smad6* mutants suggest that Smad6 could be a downstream antagonist of Bmpr2-mediated signaling in the endocardial ridges. More recently, double *Bmp6*$^{-/-}$*;Bmp7*$^{-/-}$ mutants have been shown to have hypoplastic OFT cushions. However, mechanistic interpretation of this finding was difficult as the mice seem to recover at later stages, and no OFT septation abnormalities were described (Kim et al., 2001). Our results demonstrate that modulation of the levels of BMP signaling is crucial to the development of the semilunar valves, with too much signaling (*Smad6* mutants) leading to hyperplasia, and too little (our results, *Tll1* and *Bmp6*$^{-/-}$*;Bmp7*$^{-/-}$ mutants) leading to hypoplasia of the valves.

Interestingly, mutants for molecules of the EGF signaling pathway also display enlargement of the valves, restricted to the semilunar valves (Chen et al., 2000). Antagonism of the BMP pathway by EGF signaling has previously been described in vitro (Kretzschmar et al., 1997) and activation of Ras-dependent signaling suppresses EMT (Lakkis and Epstein, 1998). Thus, the opposed phenotypes of mutants deficient in EGF (which can act through Ras mediators) and Bmpr2 signaling raise the exciting possibility that valve formation could be controlled by regulating the relative levels of signal output from Ras- and BMP-dependent pathways.

In summary, our results show that the generation of *Bmpr2* allele encoding a protein with altered signal transduction properties can reveal tissues the development of which requires wild-type levels of BMP signaling. This approach is particularly useful for studying tissues for which Cre transgenic strains are not available. Using this approach, we find that septation and valvulogenesis of the mammalian OFT is crucially dependent upon the level of BMP signaling. The finding that the OFT septation defect is restricted in *Bmpr2*$^{\Delta E2}$ mutants to the proximal region provides further genetic evidence that mechanisms of septation of the proximal and distal OFTs are distinct. Our findings show that EMT is initiated and that at least some subpopulations of cardiac neural crest cells migrate into the OFT. However, further development of the proximal OFT is impaired, most probably due to defective cell-cell interactions that depend on BMP signaling, as suggested by the downregulation of the BMP-responsive gene periostin in the OFT. The use of Cre/loxP technology will determine which cell populations require intact BMP signaling in order to mediate these important cell-cell interactions.

We are very grateful to Henry Sucov for sharing his expertise of heart development. We are indebted to E. de Robertis and Oliver Wessely for assistance with the microinjectors for the ink staining experiments. We thank Erika Bustamante, Leslie Fox, Stacey Hindy and Ray Jalian for help with genotyping, and Lisa Dornbach for cloning the periostin and Tbx1 probes. This work was supported by grants from the National Institutes of Health and the American Heart Association to K. M. L.

REFERENCES

Atkinson, C., Stewart, S., Upton, P. D., Machado, R., Thomson, J. R., Trembath, R. C. and Morrell, N. W. (2002). Primary Pulmonary Hypertension is associated with reduced pulmonary vascular expression of type II bone morphogenetic protein receptor. *Circulation* **105**, 1672-1678.

Beppu, H., Minowa, O., Miyazono, K. and Kawabata, M. (1997). cDNA cloning and genomic organization of the mouse BMP type II receptor. *Biochem. Biophys. Res. Commun.* **235**, 499-504.

Beppu, H., Kawabata, M., Hamamoto, T., Chytil, A., Minowa, O., Noda, T. and Miyazono, K. (2000). BMP type II receptor is required for gastrulation and early development of mouse embryos. *Dev. Biol.* **221**, 249-258.

Botta, A., Amati, F. and Novelli, G. (2001) Causes of the phenotype-genotype dissociation in DiGeorge syndrome: clues from mouse models. *Trends Genet.* **17**, 551-554.

Brown, C. B., Feiner, L., Lu, M.-M., Li, J., Ma, X., Webber, A. L., Jia, L., Raper, J. A. and Epstein, J. A. (2001). PlexinA2 and semaphorin signaling during cardiac neural crest development. *Development* **128**, 3071-3080.

Candia, A. F., Watabe, T., Hawley, S. H. B., Onichtchouk, D., Zhang, Y., Derynck, R., Niehrs, C. and Cho, K. W. Y. (1997). Cellular interpretation of multiple TGF-β signals: intracellular antagonism between activin/BVg1 and BMP-2/4 signaling mediated by Smads. *Development* **124**, 4467-4480.

Chen, B., Bronson, R. T., Klaman, L. D., Hampton, T. G., Wang, J., Green, P. J., Magnuson, T., Douglas, P. S., Morgan, J. P. and Neel, B. G. (2000). Mice mutant for Egfr and Shp2 have defective cardiac semilunar valvulogenesis. *Nat. Genet.* **24**, 296-299.

Chen, Y.-G., Hata, A., Lo, R. S. and Wooton, D. (1998). Determinants of specificity in TGF-β signal transduction. *Genes Dev.* **12**, 2144-2152.

Christiansen, J. H., Coles, E. G. and Wilkinson, D. G. (2000). Molecular control of neural crest formation, migration and differentiation. *Curr. Opin. Cell Biol.* **12**, 719-724.

Clark, T. G., Conway, S. J., Scott, I. C., Labosky, P. A., Winnier, G., Bundy, J., Hogan, B. L. M. and Greenspan, D. S. (1999). The mammalian tolloid-like 1 gene, *Tll1*, is necessary for normal septation and positioning of the heart. *Development* **126**, 2631-2642.

Conway, S. J., Henderson, D. J. and Copp, A. J. (1997). *Pax3* is required for cardiac neural crest migration in the mouse: evidence from the *splotch* (Sp^{2H}) mutant. *Development* **124**, 505-514.

Conway, S. J., Bundy, J., Chen, J., Dickman, E., Rogers, R. and Will, B. M. (2000). Decreased neural crest stem cell expansion is responsible for the conotruncal heart defects within the *Splotch* (*Sp*^{2H})/*Pax3* mouse mutant. *Cardiovasc. Res.* **47**, 314-328.

Daluiski, A., Engstrand, T., Bahamonde, M. E., Gamer, L. W., Agius, E., Stevenson, S. L., Cox, K., Rosen, V. and Lyons, K. M. (2001). Bone morphogenetic protein-3 is a negative regulator of bone density. *Nat. Genet.* **27**, 84-88.

Délot, E., Kataoka, H., Goutel, C., Yan, Y. L., Postlethwait, J., Wittbrodt, J. and Rosa, F. M. (1999) The BMP-related protein Radar: a maintenance factor for dorsal neuroectoderm cells? *Mech. Dev.* **85**, 15-25.

Deng, Z., Morse, J. H., Slager, S. L., Cuervo, N., Moore, K. J., Venetos, G., Kalachikov, S., Cayanis, E., Fischer, S. G., Barst, R. et al. (2000). Familial primary pulmonary hypertension (gene *PPH1*) is caused by mutations in the bone morphogenetic protein receptor-II gene. *Am. J. Hum. Genet.* **67**, 737-744.

Emanuel, B. S., Budarf, M. L. and Scambler, P. J. (1999). The genetic basis of conotruncal cardiac defects: the chromosome 22q11.2 deletion. In *Heart Development* (ed. R. P. Harvey and N. Rosenthal), pp. 463-478. San Diego, CA: Academic Press.

Epstein, J. A., Li, J., Lang, D., Chen, F., Brown, C. B., Jin, F., Lu, M. M., Thomas, M., Liu, E.-C., Wessels, A. and Lo, C. W. (2000). Migration of cardiac neural crest cells in *Splotch* mutants. *Development* **127**, 1869-1878.

Galvin, K. M., Donovan, M. J., Lynch, C. A., Meyer, R. I., Paul, R. J., Lorenz, J. N., Fairchild-Huntress, V., Dixon, K. L., Dunmore, J. H., Gimbrone, M. A., Jr et al. (2000). A role for Smad6 in development and homeostasis of the cardiovascular system. *Nat. Genet.* **24**, 171-174.

Gamer, L. W., Cox, K. A., Small, C. and Rosen, V. (2001). *Gdf11* is a negative regulator of chondrogenesis and myogenesis in the developing chick limb. *Dev. Biol.* **229**, 407-420.

Garg, V., Yamagishi, C., Hu, T., Kathiriya, I. S., Yamagishi, H. and Srivastava, D. (2001). *Tbx1*, a DiGeorge syndrome candidate gene, is regulated by Sonic Hedgehog during pharyngeal arch development. *Dev. Biol.* **235**, 62-73.

Greenwald, J., Fischer, W. H., Wale, W. W. and Choe, S. (1999). Three-finger fold for the extracellular ligand-binding domain of the type II activin receptor serine kinase. *Nat. Struct. Biol.* **6**, 18-22.

Guimond, A., Sulea, T., Pepin, M.-C. and O'Connor-McCourt, M. (1999). Mapping of putative binding sites on the ectodomain of the type II TGF-β receptor by scanning-deletion mutagenesis and knowledge-based modeling. *FEBS Lett.* **456**, 79-84.

Gurdon, J. B. and Bourillot, P. Y. (2001). Morphogen gradient interpretation. *Nature* **413**, 797-803.

Hogan, B. M. L., Beddington, R. S. P., Costantini, F. and Lacy, E. (1994). *Manipulating the Mouse Embryo*. Cold Spring Harbor, NY: Cold Spring Harbor Laboratory Press.

Hogan, B. M. L. (1996). Bone morphogenteic proteins: multifunctional regulators of vertebrate development. *Genes Dev.* **10**, 1580-1594.

Jacobs, M. L. (2000). Congenital heart surgery nomenclature and database project: truncus arteriosus. *Ann. Thorac. Surg.* **69**, S50-S55.

Ji, X., Chen, D., Xu, C., Harris, S. E., Mundy, G. R. and Yoneda, T. (2000). Patterns of gene expression associated with BMP-2-induced osteoblast and adipocyte differentiation of mesenchymal progenitor cell 3T3-F442A. *J. Bone Miner. Metab*. **18**, 132-139.

Jiang, X., Rowitch, D. H., Soriano, P., McMahon, A. P. and Sucov, H. M. (2000). Fate of the mammalian cardiac neural crest. *Development* **127**, 1607-1616.

Jones, C. M., Lyons, K. M. and Hogan, B. L. M. (1991). Involvement of *bone morphogenetic protein-4* (BMP-4) and *Vgr-1* in morphogenesis and neurogenesis in the mouse. *Development* **111**, 531-542.

Kim, S. K., Solloway, M. J. and Robertson, E. J. (2001). Bmp6 and Bmp7 are required for cushion formation and septation in the developing mouse heart. *Dev. Biol.* **235**, 449-466.

Kirby, M. L. (1999). Contribution of neural crest to heart and vessel morphology. In *Heart Development* (ed. R. Harvey and N. Rosenthal), pp. 179-193. San Diego, CA: Academic Press.

Kothapalli, D., Frazier, K. S., Welply, A., Segarini, P. R. and Grotendorst, G. R. (1997). Transforming growth factor beta induces anchorage-independent growth of NRK fibroblasts via a connective tissue growth factor-dependent signaling pathway. *Cell Growth Differ.* **8**, 61-68.

Kretzschmar, M., Doody, J. and Massagué, J. (1997). Opposing BMP and EGF signaling parthways converge on the TGF-β family mediator Smad1. *Nature* **389**, 618-622.

Kruzynska-Frejtag, A., Machnicki, M., Rogers, R., Markwald, R. R. and Conway, S. J. (2001). Periostin (an osteoblast-specific factor) is expressed within the embryonic mouse heart during valve formation. *Mech. Dev*. **103**, 183-188.

Kubalak, S. W., Hutson, D. R., Scott, K. K. and Shannon, R. A. (2002). Elevated transforming growth factor β2 enhances apoptosis and contributes to abnormal outflow tract and aortic sac development in retinoic X receptor α knockout embryos. *Development* **129**, 733-746.

Lakkis, M. H. and Epstein, J. A. (1998). Neurofibromin modulation of ras activity is required for normal endocardial-mesenchymal transformation in the developing heart. *Development* **125**, 4359-4367.

Lane, K. B., Machado, R. D., Pauciulo, M. W., Thomson, J. R., Philips, J. A., III, Loyd, J. E., Nichols, W. C. and Trembath, R. C. (2000). Heterozygous germline mutations in *BMPR2*, encoding a TGF-β receptor, cause familial primary pulmonary hypertension. The International PPH Consortium. *Nat. Genet.* **26**, 81-84.

Liu, F., Ventura, F., Doody, J. and Massagué, J. (1995). Human type II receptor for bone morphogenic proteins (BMPs): extension of the two-kinase receptor model to the BMPs. *Mol. Cell. Biol.* **15**, 3479-3486.

Liu, Y. H., Ma, L., Wu, L. Y., Luo, W., Kundu, R., Sangiorgi, F., Snead, M. L. and Maxson, R. (1994). Regulation of the msx2 homeobox gene during mouse embryogenesis: a transgene with 439 bp of 5′ flanking sequence is expressed exclusively in the apical ectodermal ridge of the developing limb. *Mech. Dev.* **48**, 187-197.

Lyons, K. M. and Hogan, B. L. M. (1993). The DVR gene family in embryonic development. In *Cell-cell Signaling in Vertebrate Development* (ed. E. J. Robertson, F. Maxfield and H. Vogel), pp. 125-137. San Diego, CA: Academic Press.

Lyons, K. M., Hogan, B. L. M. and Robertson, E. J. (1995). Colocalization of BMP 7 and BMP 2 RNAs suggests that these factors cooperatively mediate tissue interactions during murine development. *Mech. Dev.* **50**, 71-83.

Machado, R. D., Pauciulo, M. W., Thomson, J. R., Lane, K. B., Morgan, N. V., Wheeler, L., Phillips, J. A., III, Newman, J., Willliams, D., Galiè, N. et al. (2001). *BMPR2* haploinsufficiency as the inherited molecular mechanism for primary pulmonary hypertension. *Am. J. Hum. Genet.* **68**, 92-102.

Macías-Silva, M., Hoodless, P. A., Tang, S. J., Buchwald, M. and Wrana, J. L. (1998). Specific activation of smad1 signaling pathways by the BMP7 type I receptor, ALK2. *J. Biol. Chem.* **273**, 25628-25636.

Matzuk, M. M., Kumar, T. R. and Bradley, A. (1995a). Different phenotypes for mice deficient in either activins of activin receptor type II. *Nature* **374**, 356-360.

Matzuk, M. M., Lu, N., Vogel, H., Sellheyer, K., Roop, D. R. and Bradley, A. (1995b). Multiple defects and perinatal death in mice deficient in follistatin. *Nature* **374**, 360-363.

McPherron, A. C., Lawler, A. M. and Lee, S. J. (1999). Regulation of anterior/posterior patterning of the axial skeleton by growth/differentiation factor 11. *Nat. Genet.* **22**, 260-264.

Merscher, S., Funke, B., Epstein, J. A., Heyer, J., Puech, A., Lu, M. M., Xavier, R. J., Demay, M. B., Russell, R. G., Factor, S. et al. (2001). *TBX1* is responsible for cardiovascular defects in Velo-Cardio-Facial/DiGeorge syndrome. *Cell* **104**, 619-629.

Nakajima, Y., Yamagishi, T., Hokari, S. and Nakamura, H. (2000). Mechanisms involved in valvuloseptal endocardial cushion formation in

early cardiogenesis: roles of transforming growth factor (TGF)-β and bone morphogenetic proteins. *Anat. Rec.* **258**, 119-127.

Nohno, T., Ishikawa, T., Saito, T., Hosokawa, K., Noji, S., Wolsing, D. H. and Rosenbaum, J. S. (1995). Identification of a human type II receptor for bone morphogenetic protein-4 that forms differential heteromeric complexes with bone morphogenetic protein type I receptors. *J. Biol. Chem.* **270**, 22522-22526.

Oh, S. P. and Li, E. (1997). The signaling pathway mediated by the type IIB activin receptor controls axial patterning and lateral asymmetry in the mouse. *Genes Dev*. **11**, 1812-1826.

Pexieder, T. (1995). Conotruncus and its septation at the advent of the molecular biology era. In *Developmental Mechanisms of Heart Disease* (ed. E. Clark, R. Markwald and A. Takao), pp. 227-247. Armonk, NY: Futura Publishing.

Piek, E., Afrakhte, M., Sampath, K., van Zoelen, E. J., Heldin, C.-H. and ten Dijke, P. (1999). Functional antagonism between activin and osteogenic protein-1 in human embryonal carcinoma cells. *J. Cell Physiol.* **180**, 141-149.

Ramirez-Solis, R., Davis, A. C. and Bradley, A. (1993). Gene targeting in embryonic stem cells. *Methods Enzymol*. **225**, 855-878.

Roelen, B., Goumans, M.-J., van Rooijen, M. and Mummery, C. (1997). Differential expression of BMP receptors in early mouse development. *Int. J. Dev. Biol.* **41**, 541-549.

Rosenzweig, B. L., Imamura, T., Okadome, T., Cox, G. N., Yamashita, H., ten Dijke, P., Heldin, C.-H. and Miyazono, K. (1995). Cloning and characterization of a human type II receptor for bone morphogenetic proteins. *Proc. Natl. Acad. Sci. USA* **92**, 7632-7636.

Rudarakanchana, N., Flanagan, J. A., Chen, H., Upton, P. D., Machado, R., Patel, D., Trembath, R. C. and Morrell, N. W. (2002). Functional analysis of bone morphogenetic protein type II receptor mutations underlying primary pulmonary hypertension. *Hum. Mol. Genet.* **11**, 1517-1525.

Scott, I. C., Blitz, I. L., Pappano, W. N., Imamura, Y., Clark, T. G., Steiglitz, B. M., Thomas, C. L., Maas, S. A., Takahara, K., Cho, K. W. and Greenspan, D. S. (1999). Mammalian BMP-1/Tolloid-related metalloproteinases, including novel family member mammalian Tolloid-like 2, have differential enzymatic activities and distributions of expression relevant to patterning and skeletogenesis. *Dev. Biol.* **213**, 283-300.

Solloway, M. J., Dudley, A. T., Bikoff, E. K., Lyons, K. M., Hogan, B. L. M. and Robertson, E. J. (1998). Mice lacking *Bmp6* function. *Dev. Genet.* **22**, 321-339.

Storm, E. E. and Kingsley, D. M. (1996). Joint patterning defects caused by single and double mutations in members of the bone morphogenetic protein (BMP) family. *Development* **122**, 3969-3979.

ten Dijke, P., Yamashita, H., Sampas, T. K., Reddi, A. H., Estevez, M., Riddle, D. L., Ichijo, H., Heldin, C.-H. and Miyazono, K. (1994). Identification of type I receptors for osteogenic protein-1 and bone morphogenetic protein-4. *J. Biol. Chem.* **269**, 16985-16988.

Thomson, J. R., Machado, R. D., Pauciulo, M. W., Morgan, N. V., Humbert, M., Elliott, G. C., Yacoub, M., Mikhail, G., Rogers, P., Newman, J. et al. (2000). Sporadic primary pulmonary hypertension is associated with germline mutations of the gene encoding BMPR-II, a receptor member of the TGF-β family. *J. Med. Genet.* **68**, 92-102.

Vitelli, F., Morishima, M., Taddei, I., Lindsay, E. A. and Baldini, A. (2002). *Tbx1* mutation causes multiple cardiovascular defects and disrupts neural crest and cranial nerve migratory pathways. *Hum. Mol. Genet.* **11**, 915-922.

Winnier, G., Blessing, M., Labosky, P. A. and Hogan, B. L. M. (1995). Bone morphogenetic protein-4 (BMP-4) is required for mesoderm formation and patterning in the mouse. *Genes Dev.* **9**, 2105-2117.

Yamashita, H., ten Dijke, P., Huylebroek, D., Sampath, T. K., Andries, M., Smith, J. C., Heldin, C.-H. and Miyazono, K. (1995). Osteogenic protein-1 binds to activin type II receptors and induces certain activin-like effects. *J. Cell Biol.* **130**, 217-226.

Zhang, H. and Bradley, A. (1996). Mice deficient for BMP2 are non viable and have defects in amnion/chorion and cardiac development. *Development* **122**, 2977-2986.